Estimating the Global Radiative Impact of the Sea-Ice-Albedo Feedback in the Arctic

Stephen R. Hudson

Norwegian Polar Institute, Tromsø, Norway

Abstract.
   A simple method for estimating the global radiative forcing caused by the sea-ice-albedo feedback in the Arctic is presented. It is based on observations of cloud cover, sea-ice concentration, and top-of-atmosphere broadband albedo. The method does not rely on any sort of climate model, making the assumptions and approximations clearly visible and understandable, and allowing them to be easily changed. Results show that the globally and annually averaged radiative forcing caused by the observed loss of sea ice in the Arctic between 1979 and 2007 is approximately 0.1 W m^{-2}; a complete removal of Arctic sea ice results in a forcing of about 0.7 W m^{-2}, while a more realistic ice-free-summer scenario (no ice for one month, decreased ice at all other times of the year) results in a forcing of about 0.3 W m^{-2}, similar to present-day anthropogenic forcing caused by halocarbons. The potential for changes in cloud cover as a result of the changes in sea ice makes the evaluation of the actual forcing that may be realized quite uncertain, since such changes could overwhelm the forcing caused by the sea-ice loss itself, if the cloudiness increases in the summertime.

1. Introduction

   The rapid reduction in Arctic sea-ice extent observed between 2005 and 2010 and the longer term reduction observed in the prior decades [*Stroeve et al.*, 2008; *Comiso et al.*, 2008; *Parkinson and Cavalieri*, 2008] have helped bring attention to the sea-ice-albedo feedback [*Curry et al.*, 1995], both within the scientific community [e.g., *Comiso*, 2009; *Perovich et al.*, 2008, 2007a, b] and in media reports about climate change. In general introductions to the topic of climate change, the sea-ice-albedo feedback (SIAF) is often singled out for use in explaining the concept of climate feedbacks (e.g., it is the only feedback mentioned by *Gore* [2006]), something that can give the impression to the interested public that it is the most important feedback process, while its popularity likely stems from the relative ease with which it can be explained and grasped.
   Locally and regionally, the SIAF is a very important component of the Arctic climate system [e.g., *Perovich et al.*, 2007a; *Hall*, 2004]. Here, its global importance is considered by estimating the global, annually averaged, radiative effect of the observed, and possible future, loss of sea ice in the Arctic, allowing a comparison of the radiative forcing caused by the Arctic sea-ice melt with direct climate forcings, such as those presented by the IPCC [*Forster et al.*, 2007]. There have

been previous studies to examine the global impact of the albedo feedback [some examples from five decades, *Lian and Cess*, 1977; *Wang and Stone*, 1980; *Ingram et al.*, 1989; *Covey et al.*, 1991; *Hall*, 2004; *Flanner et al.*, 2011]. The methods used in these studies have varied, but the first five all rely on some form of a global climate model, with the effect of the albedo decrease due to loss of sea ice or sea ice and snow isolated to some extent; of these five, only one [*Covey et al.*, 1991] gives a result as a global radiative forcing, while the three earlier studies report either a relative change in the climate sensitivity or a feedback parameter (the change in radiative forcing per unit change in temperature), and *Hall* [2004] presents geographically distributed temperature changes. The last study [*Flanner et al.*, 2011] is more similar to this one, but focuses on both snow and sea ice, and uses very different methods, allowing for an interesting comparison of their results with the results here, presented in Section 4.
   This study focuses directly on the changes in the amount of solar radiation absorbed by Earth due to the loss of Arctic sea ice. It focuses only on the Arctic because that is where significant changes have been observed in recent decades. The estimates here are based mostly on observations, rather than on the results of climate models. Furthermore, they are kept relatively simple, to make the uncertainties and assumptions that go into the calculation of the increased absorption of solar radiation as clear as possible. This method does not provide the possibility to give a detailed assessment of the specific changes in regional temperature or other variables, and it is, therefore, a complement to, rather than a replacement for, studies with complex climate

models, such as that presented by *Hall* [2004]. The results are presented as radiative forcing (W m^{-2}) for a given change in sea ice, rather than as a feedback parameter (W m^{-2} K^{-1}), because of the nonlinear nature of the SIAF, which decreases in effectiveness as the amount of sea ice in the sunlit season decreases towards zero.

2. Method

The method aims to isolate the effect of the decrease in albedo caused by a given decrease in sea ice coverage, and to be simple and clear enough to allow it to be changed as new or better data, approximations or assumptions become available. As the goal is to examine the global effect of the SIAF, the focus is on albedo changes at the top of the atmosphere (TOA). The basic outline is: 1) a grid is set up that covers all areas of the Northern Hemisphere that may have sea ice cover at some point in the year; 2) data are obtained to estimate the sea-ice concentration and cloud fraction in each grid cell, as a function of time of year; 3) data are obtained to estimate the TOA albedo, as a function of solar zenith angle, for clear and cloudy sky over sea ice and over ocean; 4) the solar zenith angle is calculated as a function of time and latitude (with a program adapted by Warren Wiscombe from *Michalsky* [1988]); 5) for each time interval through the year, the energy absorbed in each grid cell is calculated as

$$
\begin{aligned}
E_{\mathrm{abs}} = S_{\mathrm{o}} \, \cos(\theta_{\mathrm{o}}) \, A \, \Delta t \, \Big\{ & [1 - \alpha_{\mathrm{cldI}}(\theta_{\mathrm{o}}, M)] \, [f_{\mathrm{i}} \, f_{\mathrm{c}}] \\
& + [1 - \alpha_{\mathrm{clrI}}(\theta_{\mathrm{o}}, M)] \, [f_{\mathrm{i}} \, (1 - f_{\mathrm{c}})] \\
& + [1 - \alpha_{\mathrm{cldO}}(\theta_{\mathrm{o}})] \, [(1 - f_{\mathrm{i}}) \, f_{\mathrm{c}}] \\
& + [1 - \alpha_{\mathrm{clrO}}(\theta_{\mathrm{o}})] \, [(1 - f_{\mathrm{i}}) \, (1 - f_{\mathrm{c}})] \Big\},
\end{aligned}
\tag{1}
$$

where S_{o} is the solar flux at the TOA (set to 1365 W m^{-2}), θ_{o} is the solar zenith angle, A is the area of the grid cell, Δt is the time step (150 s), α_{cldI}, α_{clrI}, α_{cldO}, and α_{clrO} are the broadband TOA albedos for cloud over sea ice, clear sky over sea ice, cloud over ocean, and clear sky over ocean, respectively, and f_{i} and f_{c} are the fractions of the grid cell with sea ice (ice concentration) and cloud (cloud fraction). In addition to the albedos being a function of θ_{o}, the sea-ice albedos are a function of whether the sea ice is assumed to be melting or not, as indicated in the equation by M, a binary test for melting, which affects which $\alpha_{\mathrm{cldI}}(\theta_{\mathrm{o}})$ and $\alpha_{\mathrm{clrI}}(\theta_{\mathrm{o}})$ curves are used. Equation 1 is evaluated for each ocean grid cell, for each 2.5-minute time step through the year, and the total energy absorbed ($E_{\mathrm{abs}}^{\mathrm{Tot}}$) is calculated by summing over all grid cells and time steps. This is done for different scenarios, which differ in their prescribed progression of f_{i} with time in each grid cell (the progression of f_{c} can also be changed); the final result, the change in radiative forcing due to the change in f_{i} is then determined by dividing the difference between $E_{\mathrm{abs}}^{\mathrm{Tot}}$ in a pair of scenarios by the surface area of Earth (set to 5.10072×10^{14} m^2) and by 3.1536×10^7 s (1 year) to convert it to W m^{-2}. As seen in Equation 1, within each grid cell, random overlap of clouds and sea ice is assumed.

Historical values of f_{i} are from gridded monthly sea-ice concentrations determined from passive microwave satellite data [*Cavalieri et al.*, 1996, updated 2008]. These data were obtained for all months from

January 1979 to December 2007. The data gap around the pole is filled using bilinear interpolation. The grid used in this dataset is also used for the calculations presented here. It covers 7.56×10^7 km^2 of the Northern Hemisphere, of which 3.74×10^7 km^2 is ocean, including some ocean never covered by sea ice; see the supplementary material for more information about the grid. For each month, the monthly concentration field from the dataset is used as the concentration field on the fifteenth of that month; the fields on other days are then linearly interpolated at each grid cell. All forcings are presented as anomalies from the absorption calculated with the 1979–1998 climatological (monthly-varying) ice field. The climatological ice concentration field, along with the domain and land mask can be viewed in the animation with the supplementary material.

Historical values of f_{c} are from the the cloud climatology presented by *Hahn and Warren* [2007], which is based on synoptic weather observations that reported cloud cover and type, made between 1954 and 1997. From this climatology, the zonally and seasonally averaged total cloud fractions, based on combined day and night data from ocean observations only, were used. *Hahn and Warren* do provide longitudinally varying values; however the longitudinal grid spacing varies in the Arctic (to keep approximately constant grid-box area), and not all grid boxes have data for all seasons. These issues, combined with the weak longitudinal variations in the sea-ice areas, especially in summer, prompted the decision to use the zonal means. *Hahn and Warren* give these values for 5° latitude bands, and these were interpolated linearly in latitude to get f_{c} at each grid location; no interpolation in time was done (the winter value was used for all of Dec, Jan, and Feb, etc.). Figure 1 shows the cloud fractions used here for each season, as a function of latitude.

The TOA albedos α_{clrI}, α_{cldI}, and α_{clrO} are from the average broadband albedo for these scene types observed by the Clouds and the Earth's Radiant Energy System (CERES) satellite instruments during the
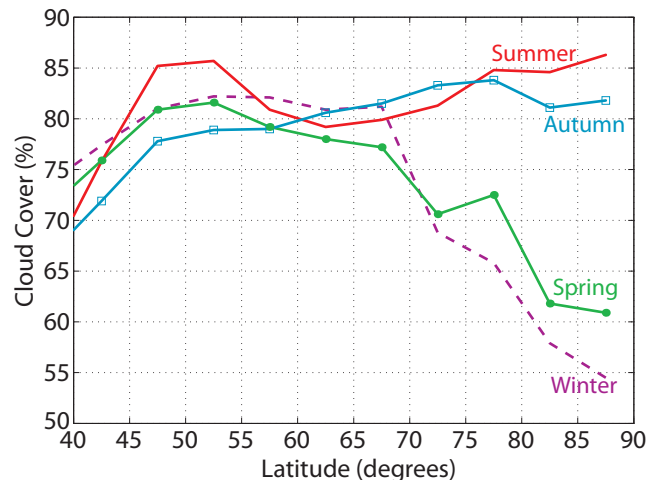

Figure 1. The percentage of cloud cover used in this work, as a function of latitude, for each of the four seasons is shown. Data are taken from *Hahn and Warren* [2007].

two-year period used for the development of their snow and sea-ice angular distribution models. The method used to determine these scene-dependent albedos as a function of solar zenith angle is described by *Kato and Loeb* [2005]. *Kato and Loeb* separated sea-ice scenes into bright and dark sea ice, which turned out to correspond well with melting and non-melting surfaces; this gives two possible curves to use for both $\alpha_{\mathrm{clrI}}(\theta_\circ)$ and $\alpha_{\mathrm{cldI}}(\theta_\circ)$. This distinction is used here to try to include the part of the SIAF that acts before the complete disappearance of the ice, as melting snow and melt ponds darken the surface. In the calculations here, from 1 Jul to 31 Aug, approximately the melt period in the central Arctic [*Markus et al.*, 2009], the dark-ice albedo is used in all grid cells; at other times, the dark-ice albedo is used in grid cells with less than 25% ice concentration, or where the ice concentration decreases by more than 10% from one month to the next (if the decrease occurs from Apr to May, the dark albedo is used from 16 Apr to 15 May); otherwise the bright-ice albedo is used. This stepwise change in albedo is a significant simplification from the real progression of sea-ice albedo, which changes with the onset of snowmelt, the loss of snow, the formation and maturation of melt ponds, among other things [*Perovich et al.*, 2002, 2007b], but it is an improvement over ignoring such changes altogether. *Kato and Loeb* give the albedos in 5° bins of $\theta_\circ$, and these values are linearly interpolated to values appropriate for the latitude of each grid cell at the given time step. The CERES albedos can be downloaded from http://asd-www.larc.nasa.gov/Inversion/adm/terra-adm-snow.html.

The albedo curves for cloud over sea ice, are the average of the thick and thin cloud scenes in the CERES dataset.

Kato and Loeb [2005] did not give albedos for overcast scenes over open water, so $\alpha_{\mathrm{cldO}}(\theta_\circ)$ is taken from the results of a radiative transfer model. The model, SBDART [Santa Barbara DISORT Atmospheric Radiative Transfer Model; *Ricchiazzi et al.*, 1998], was used to calculate the broadband (integrated over wavelengths from 0.2 to 10 μm, with thermal emission turned off) TOA albedo over the standard subarctic summer atmosphere [*McClatchey et al.*, 1972], with a cloud with optical thickness 10 (the median optical thickness found over sea ice in the CERES dataset [*Kato and Loeb*, 2005], and in line with previous findings for summertime Arctic clouds [*Curry et al.*, 1996]) and droplet radius 10 μm placed between 1 and 2 km, and with the surface reflectance described using SBDART's built in ocean water bidirectional reflectance distribution function; it was run at 5° intervals in $\theta_\circ$, and the resulting albedos were linearly interpolated to values appropriate for the latitude of each grid cell at the given time step.

Figure 2 shows the six albedo curves used in the calculation. Since solar zenith angles over sea ice are almost never less than about 35 degrees, the CERES dataset does not give sea-ice albedos for these small zenith angles; if they were needed in the calculation, the albedo for the smallest available solar zenith angle was used. The fact that the cloud-over-ocean albedo becomes larger than the clear-ice albedo at moderate solar zenith angles is likely due to the fact that most
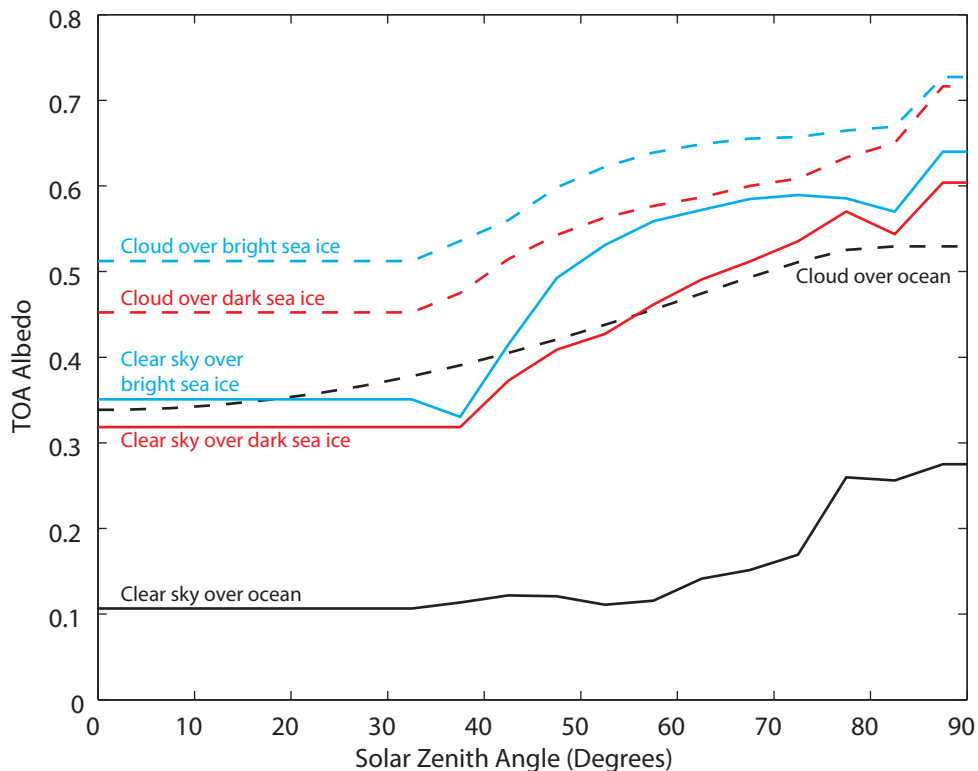

Figure 2. The six albedo curves, as functions of the solar zenith angle, that were used in this calculation. Dashed curves are for cloudy scenes, solid for clear scenes; cyan curves are for bright sea ice, red for dark sea ice, and black for open ocean. All curves except that for cloud over ocean are from data presented by *Kato and Loeb* [2005].
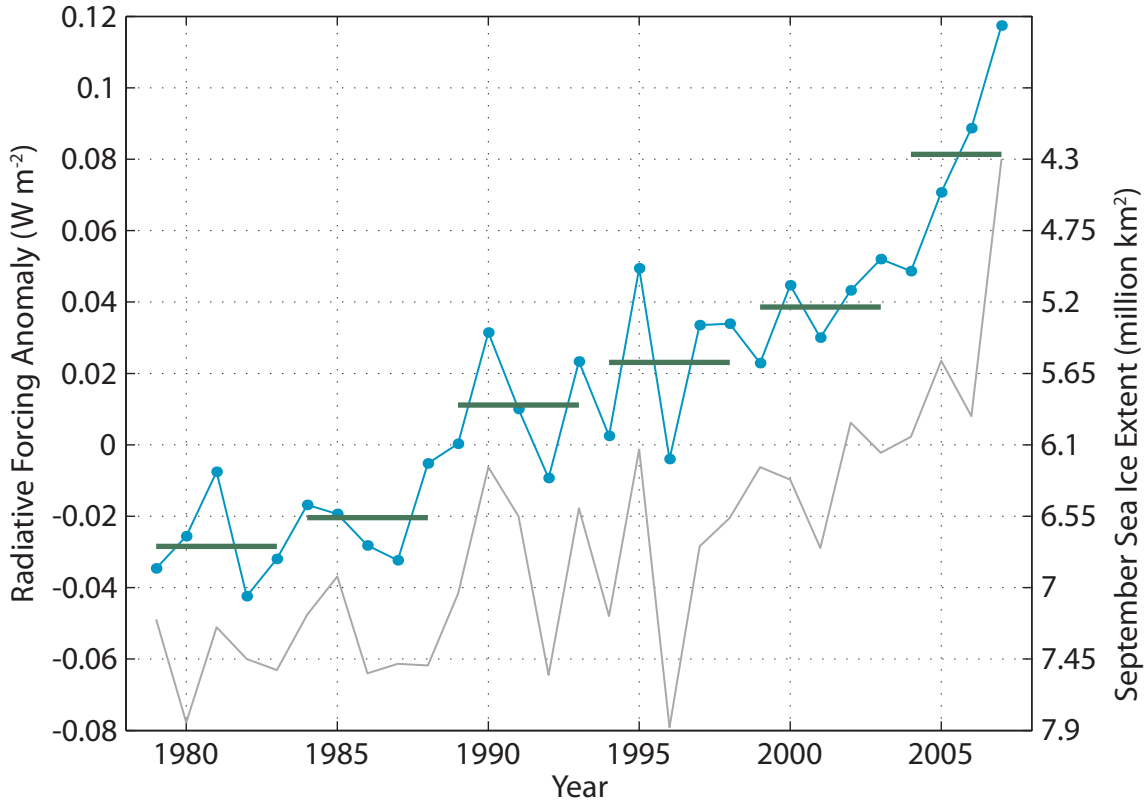
Figure 3. The top series (line with dots) shows the yearly anomalies in globally and annually averaged radiative forcing caused by that year's anomalies in Arctic sea-ice area. All anomalies are from the 1979–1998 20-year mean. The horizontal lines give 5-year averages of the radiative forcing anomalies (4 years for the last one because 2008 ice concentration data were not yet finalized). The lower series, plotted against the right-hand axis, is the mean Arctic sea-ice extent in September of each year, with the scale inverted.

sea ice under solar zenith angles less than 50 degrees has already undergone some significant surface melt, darkening the surface. The deviation from a monotonic increase in the sea-ice albedo curves could illustrate uncertainties in the data, or they could reflect the competing factors affecting the TOA albedo, i.e., as the solar zenith angle increases, the surface albedo increases (increasing the TOA albedo), but the atmospheric absorption also increases (decreasing the TOA albedo).

3. Results

For each year from 1979 to 2007, the energy absorbed with the observed ice concentration field was compared to that with the 1979–1998 climatological ice concentration field to determine the radiative forcing resulting from the deviations from climatology of the ice concentration in that year. The resulting time series of radiative forcing is shown in Figure 3. While similar to the inverse of the commonly seen plot of September ice extent versus time, it differs from this in that Figure 3 is not based on ice anomalies at any one time of year, but is an integration over the whole year, with the most weight on ice changes when and where there is significant solar insolation, i.e. in May, Jun, and Jul, and at lower latitudes in other months.

It is also interesting to consider possible forcing caused by any continued loss of Arctic sea ice in the future. If all sea ice is removed from all grid cells

throughout the entire year, the calculation results in an additional radiative forcing of 0.68 W m^{-2}, compared with the climatological ice concentration. This value can be seen as an estimate of the upper limit of the direct effect of the SIAF caused by Arctic sea-ice melt. It is, however, an unrealistic scenario for the coming decades, when ice will likely reform in winter, even if it begins to entirely melt away in the summer.

A more realistic scenario [e.g., *Boé et al.*, 2009], with an Arctic that is free of sea ice for one month in late summer, can be used to estimate the radiative forcing the SIAF in the Arctic may cause during coming decades. This scenario was constructed for this work, based on the observed 2007 ice concentration, shifted to make the period from 15 Aug to 15 Sep ice-free. In this scenario, the mid-month ice concentration fields from Oct to Mar are set to the monthly mean fields from Sep to Feb 2007, and the mid-month fields from Apr to Jul are set to the monthly mean fields from May to Aug 2007; the mid-month ice concentration was set to zero everywhere in Aug and Sep, with the usual linear interpolation between the 15 Jul and 15 Aug fields (the melt-off over the whole region that still had ice in Aug 2007) and between the 15 Sep and 15 Oct fields (the formation of new ice over the whole region that had ice in Sep 2007). This ice concentration field is also shown in the animation with the supplementary material. It is a hypothetical progression of the distribution of sea

ice in a somewhat warmer climate, not an attempt to predict it exactly at any given point in the future, or for any given amount of warming.

Using this ice-free-summer scenario, the estimated radiative forcing caused by the albedo reduction due to the lost ice is 0.29 W m^{-2}. This provides a more realistic idea of the potential impact of the SIAF caused by changes to Arctic sea ice that are predicted to occur this century by many GCMs.

4. Discussion

Despite the fact that the two studies used very different methods, the results presented here agree quite well with results presented by *Flanner et al.* [2011]. Their central estimate of cooling caused by Arctic sea ice is 0.65 W m^{-2}, compared to 0.68 W m^{-2} in this study (numbers given by *Flanner et al.* are averaged over the area of the Northern Hemisphere, rather than the entire planet, and must therefore be divided by 2 for comparison with numbers presented here). Likewise, their estimate of reduced cooling caused by sea-ice loss from 1979 to 2008, about 0.11 W m^{-2}, is similar to the change shown in Figure 3.

The results presented here are intended to assess the effect of one process, the SIAF, in isolation, and in a way in which the uncertainties and assumptions are clearly visible and easily changed. In the remainder of this section, some of the uncertainties are discussed, along with the main complexity associated with assessing the radiative forcing caused by sea-ice melt.

There are uncertainties in all three data sources: the historical ice concentrations, the TOA albedo functions, and the cloud climatology.

Ice concentration estimates from passive microwave data are known to underestimate the concentration during the melt season, when melt ponds and wet ice are mistaken for open water [*Andersen et al.*, 2007; *Meier*, 2005]. This may cause the calculations presented here to underestimate the forcing by reducing the area covered by sea ice in the climatology. The exact bias in the passive microwave data is difficult to quantify, and varies with season, but both *Andersen et al.* [2007] and *Meier* [2005] reported negative biases in some cases of up to about 15%. To find a bound on the possible effect of this bias in the calculation here, the ice-free-summer scenario was rerun, with increased ice in the areas estimated to be melting (in both the climatological and ice-free-summer fields). Specifically, where it was determined to use the dark ice albedo, f_i was increased by 15% where $0\% < f_i < 80\%$, and was increased to 95% where $80\% \leq f_i < 95\%$. With these increses in f_i, the calculated forcing caused by a shift to the ice-free-summer scenario increased to 0.37 W m^{-2}, from 0.29 W m^{-2}. Taking nearly the maximum bias over all metlting areas probably provides an upper bound for the effect of this uncertainty on the calculation here.

The TOA albedos are mostly based on a modern set of observations of broadband albedo at the TOA, with good scene identification; however, using only six curves for $\alpha(\theta_\circ)$ is clearly a significant simplification, especially for the cloud-covered area, where the albedo will obviously vary with cloud thickness and other physical properties. While this is a simplification, trying to add more scene types, either with varying cloud properties or more types of sea ice, would greatly reduce

the transparency of the method, without necessarily improving the result. On the other hand, CERES is still a fairly new dataset and the *Kato and Loeb* [2005] albedo data were not developed specifically as a climatological albedo dataset. The CERES project will likely result in better albedo datasets in the future, which, once available, could be used to improve this type of calculation.

To examine the uncertainty due to the prescribed albedos, the radiative forcing caused by a change to the ice-free-summer scenario was calculated eight more times; each time, the albedo curve for one scene type was increased or decreased by 10% (relative change). Table 1 shows the resulting radiative forcing for each case, giving a range of possible forcings of 0.21 to 0.36 W m^{-2}. The calculation is most sensitive to changes in the albedo of cloudy scenes. *Kato and Loeb* [2005] estimate RMS errors for their retrieved fluxes over sea-ice scenes of up to about 6%, excluding errors caused by sensor calibration uncertainties and scene identification error; therefore, 10% seems like a reasonable level of uncertainty for the albedos overall.

The cloud cover climatology is based on visual observations made from ships, eliminating the problems associated with identifying clouds over the Arctic with satellite observations. The largest source of uncertainty related to the clouds is that in this study no interannual variability or future cloud changes were included. This brings up what is likely the biggest problem associated with understanding the SIAF: isolating its effects from cloud changes.

The frequent cloud cover in the Arctic, especially in summer, reduces the global radiative effect of removing sea ice. Therefore, any changes in cloudiness that happen concurrently with changes in sea ice, whether as a cause or effect, will significantly alter the overall radiative forcing caused by the sea ice changes. While considering the potential cloud changes makes the results no longer entirely focused on the SIAF, it is worth

Table 1. Radiative forcing caused by a change from the climatological ice concentration field to the ice-free-summer field, calculated with a variety of changes to the prescribed albedos and cloud cover. The value in the first row was calculated with the standard albedo curves and cloud climatology; each of the other results was calculated with one albedo curve changed as indicated, or with a change to the cloud fraction. When albedos for ice scenes were changed, both the bright- and dark-ice curves were changed simultaneously. Except for the last two rows, the indicated changes were made with both the climatological and ice-free-summer cases; for the final two rows, the clouds were changed only in the ice-free-summer case.

Case	Forcing (W m^{-2})
Unchanged	0.29
$\alpha_{\mathrm{clrO}} + 10\%$	0.28
$\alpha_{\mathrm{clrO}} - 10\%$	0.29
$\alpha_{\mathrm{clrI}} + 10\%$	0.30
$\alpha_{\mathrm{clrI}} - 10\%$	0.27
$\alpha_{\mathrm{cldO}} + 10\%$	0.23
$\alpha_{\mathrm{cldO}} - 10\%$	0.35
$\alpha_{\mathrm{cldI}} + 10\%$	0.36
$\alpha_{\mathrm{cldI}} - 10\%$	0.21
$f_{\mathrm{c}} = 0$	0.56
$f_{\mathrm{c}} + 15\%$	0.25
$f_{\mathrm{c}} - 15\%$	0.33
$f_{\mathrm{c}} + 15\%$ (IFS only)	-0.31
$f_{\mathrm{c}} - 15\%$ (IFS only)	0.89

doing to get a sense of to what degree the global effect of the SIAF can be masked by cloud-cover changes.

The effect of clouds was examined in two ways. First, to look at the result of uncertainties in the specified cloud cover, the ice-free-summer scenario was run with cloud fraction changed by $\pm15\%$ everywhere, in both the climatological ice year and the ice-free-summer year. These changes resulted in radiative forcings of $0.25\,\mathrm{W\,m^{-2}}$ with increased cloud cover and $0.33\,\mathrm{W\,m^{-2}}$ with decreased, compared to $0.29\,\mathrm{W\,m^{-2}}$ with the standard cloud climatology. This range gives an estimate of the uncertainty in this calculation due to the cloud cover uncertainties. Given that interannual variability in the cloud dataset in the Arctic Ocean is on the order of $\pm5\%$ to $\pm10\%$, depending on season [*Eastman and Warren*, 2010], this is quite a large uncertainty to impose on the cloud climatology, and still resulted in a relatively small change to the overall result.

The second cloud experiment was done to examine the possibility of the SIAF being enhanced or overwhelmed by changes in cloudiness that happen along with changes in sea ice cover. In this test, the cloud cover for the year with the climatological sea-ice cover was set to the normal cloud climatology, but the cloud cover for the ice-free-summer year was changed by $\pm15\%$. A 15% decrease in cloudiness occurring concurrently with the shift to the ice-free-summer case increases the radiative forcing to $0.89\,\mathrm{W\,m^{-2}}$, while a 15% increase in cloudiness changes even the sign of the overall radiative forcing, bringing it to $-0.31\,\mathrm{W\,m^{-2}}$. This experiment should be viewed as bounding the offsetting or enhancing effect of cloud changes. A 15% change in cloud cover is considerable, approximately twice the observed interannual variability in the Arctic Ocean, and more than 3 times the observed difference between mean cloud amount in low and high ice years during the period 1979 to 2007 [*Eastman and Warren*, 2010].

These results show that a strong sea-ice-cloud feedback could greatly enhance or completely overwhelm the global effect of the SIAF. There remains uncertainty about the likely changes in cloud cover associated with changes in sea ice, but an inverse relationship is generally expected, which would dampen the SIAF. However this relationship is expected to be weakest in summer [*Eastman and Warren*, 2010; *Kay and Gettelman*, 2009], when the SIAF is most important, minimizing the dampening effect of increased cloudiness. Clearly a better understanding of what cloud changes are likely in the Arctic is necessary for a full assessment of the SIAF.

An additional interesting investigation regarding clouds is to see to what extent the current cloud cover masks the potential SIAF. To look at this, the ice-free-summer scenario was run with no cloud cover in either the climatological ice year or the ice-free-summer year. This removal of all clouds increased the calculated radiative forcing caused by the change in sea-ice area from 0.29 to $0.56\,\mathrm{W\,m^{-2}}$, indicating that present-day cloud cover has the ability to mask approximately half of the clear-sky SIAF.

5. Conclusion

A relatively simple method of estimating the global radiative forcing due to the SIAF in the Arctic was used to show that the sea-ice loss observed between 1979 and 2007 is capable of producing a radiative forcing of about $0.11\,\mathrm{W\,m^{-2}}$, while removing all ice throughout the year would result in a radiative forcing of around $0.7\,\mathrm{W\,m^{-2}}$, slightly less than half of current total net anthropogenic forcing [*Forster et al.*, 2007]. An ice-free-summer scenario (one month with no ice, reduced ice at all other times) produced a forcing of about $0.3\,\mathrm{W\,m^{-2}}$, similar to the present-day anthropogenic forcing caused by tropospheric ozone pollution or by halocarbon emissions [*Forster et al.*, 2007].

The largest uncertainty in the future radiative forcing caused by sea-ice loss is related to how clouds in the Arctic will change. If cloud cover increases as sea ice decreases, that could offset the direct effect of the SIAF, especially if clouds increase in summer, when there is the most sun and the most sea-ice loss. However, studies so far have found that the summer season has the lowest correlation between ice cover and cloud cover, which would minimize the offsetting effect that clouds play.

References

Andersen, S., R. Tonboe, L. Kaleschke, G. Heygster, and L. T. Pedersen (2007), Intercomparison of passive microwave sea ice concentration retrievals over the high-concentration Arctic sea ice, *J. Geophys. Res.*, *112*, C08,004, doi:10.1029/2006JC003543.

Boé, J., A. Hall, and X. Qu (2009), September sea-ice cover in the Arctic Ocean projected to vanish by 2100, *Nature Geoscience*, *2*, 341–343, doi:10.1038/ngeo467.

Cavalieri, D., C. Parkinson, P. Gloersen, and H. J. Zwally (1996, updated 2008), Sea ice concentrations from Nimbus-7 SMMR and DMSP SSM/I passive microwave data, 1979–2007, National Snow and Ice Data Center, Boulder, Colorado, USA, Digital media.

Comiso, J. C. (2009), The rapidly shrinking sea ice cover and ice-albedo feedback effects, *AGU Fall Meeting Abstracts*, pp. A31A–0094.

Comiso, J. C., C. L. Parkinson, R. Gersten, and L. Stock (2008), Accelerated decline in the Arctic sea ice cover, *Geophys. Res. Lett.*, *35*, L01,703, doi:10.1029/2007GL031972.

Covey, C., K. E. Taylor, and R. E. Dickinson (1991), Upper limit for sea ice albedo feedback contribution to global warming, *J. Geophys. Res.*, *96*(D5), 9169–9174, doi:10.1029/91JD00236.

Curry, J. A., J. L. Schramm, and E. E. Ebert (1995), Sea ice-albedo climate feedback mechanism, *J. Climate*, *8*(2), 240–247, doi:10.1175/1520-0442(1995)008⟨0240:SIACFM⟩2.0.CO;2.

Curry, J. A., W. B. Rossow, D. Randall, and J. L. Schramm (1996), Overview of Arctic cloud and radiation characteristics, *J. Climate*, *9*(8), 1731–1764, doi:10.1175/1520-0442(1996)009⟨1731:OOACAR⟩2.0.CO;2.

Eastman, R., and S. G. Warren (2010), Interannual variations of Arctic cloud types in relation to sea ice, *J. Climate*, *23*(15), 4216–4232, doi:10.1175/2010JCLI3492.1.

Flanner, M. G., K. M. Shell, M. Barlage, D. K. Perovich, and M. A. Tschudi (2011), Radiative forcing and albedo feedback from the Northern Hemisphere cryosphere between 1979 and 2008, *Nature Geoscience*, *Advanced online publication*, doi:10.1038/ngeo1062.

Forster, P., et al. (2007), *Climate Change 2007: The Physical Science Basis. Contribution of Working Group I to the Fourth Assessment Report of the Intergovernmental Panel on Climate Change*, chap. Changes in Atmospheric Constituents and in Radiative Forcing, Cambridge University Press, Cambridge, United Kingdom, and New York, USA.

Gore, A. (2006), *An Inconvenient Truth*, Rodale Press, 325 pages.

Hahn, C. J., and S. G. Warren (2007), *A gridded climatology of clouds over land (1971–96) and ocean (1954–97) from surface observations worldwide*, Carbon Dioxide Information Analysis Center, Report NDP-026E, doi:10.3334/CDIAC/cli.ndp026e, 71 pp.

Hall, A. (2004), The role of surface albedo feedback in climate, *J. Climate*, *17*, 1550–1568, doi:10.1175/1520-0442(2004)017⟨1550:TROSAF⟩2.0.CO;2.

Ingram, W. J., C. A. Wilson, and J. F. B. Mitchell (1989), Modeling climate change: An assessment of sea ice and surface albedo feedbacks, *J. Geophys. Res.*, *94*(D6), 8609–8622, doi:10.1029/JD094iD06p08609.

Kato, S., and N. G. Loeb (2005), Top-of-atmosphere shortwave broadband observed radiance and estimated irradiance over polar regions from Clouds and the Earth's Radiant Energy System (CERES) instruments on Terra, *J. Geophys. Res.*, *110*, D07202, doi:10.1029/2004JD005308.

Kay, J. E., and A. Gettelman (2009), Cloud influence on and response to seasonal Arctic sea ice loss, *J. Geophys. Res.*, *114*, D18,204, doi:10.1029/2009JD011773.

Lian, M. S., and R. D. Cess (1977), Energy balance climate models: A reappraisal of ice-albedo feedback, *J. Atmos. Sci.*, *34*(7), 1058–1062, doi:10.1175/1520-0469(1977)034⟨1058:EBCMAR⟩2.0.CO;2.

Markus, T., J. C. Stroeve, and J. Miller (2009), Recent changes in arctic sea ice melt onset, freezeup, and melt season length, *J. Geophys. Res.*, *114*, C12,024, doi:10.1029/2009JC005436.

McClatchey, R. A., R. W. Fenn, J. E. A. Selby, F. E. Volz, and J. S. Garing (1972), *Optical Properties of the Atmosphere (Third Edition)*, no. 411 in Environmental Research Papers, Air Force Cambridge Research Laboratories, Bedford, Massachusetts.

Meier, W. N. (2005), Comparison of passive microwave ice concentration algorithm retrievals with AVHRR imagery in Arctic peripheral seas, *IEEE Trans. Geosci. Remote Sens.*, *43*(6), 1324–1337, doi:10.1109/TGRS.2005.846151.

Michalsky, J. J. (1988), The Astronomical Almanac's algorithm for approximate solar position (1950–2050), *Solar Energy*, *40*(3), 227–235, doi:10.1016/0038-092X(88)90045-X.

Parkinson, C. L., and D. J. Cavalieri (2008), Arctic sea ice variability and trends, 1979–2006, *J. Geophys. Res.*, *113*, C07,003, doi:10.1029/2007JC004558.

Perovich, D. K., T. C. Grenfell, B. Light, and P. V. Hobbs (2002), Seasonal evolution of the albedo of multiyear Arctic sea ice, *J. Geophys. Res.*, *107*(C10), 8044, doi:10.1029/2000JC000438.

Perovich, D. K., B. Light, H. Eicken, K. F. Jones, K. Runciman, and S. V. Nghiem (2007a), Increasing solar heating of the Arctic Ocean and adjacent seas, 1979–2005: Attribution and role in the ice-albedo feedback, *Geophys. Res. Lett.*, *34*, L19,505, doi:10.1029/2007GL031480.

Perovich, D. K., S. V. Nghiem, T. Markus, and A. Schweiger (2007b), Seasonal evolution and interannual variability of the local solar energy absorbed by the Arctic sea ice-ocean system, *J. Geophys. Res.*, *112*, C03,005, doi:10.1029/2006JC003558.

Perovich, D. K., J. A. Richter-Menge, K. F. Jones, and B. Light (2008), Sunlight, water, and ice: Extreme Arctic sea ice melt during the summer of 2007, *Geophys. Res. Lett.*, *35*, L11,501, doi:10.1029/2008GL034007.

Ricchiazzi, P., S. Yang, C. Gautier, and D. Sowle (1998), SBDART: A research and teaching software tool for plane-parallel radiative transfer in the Earth's atmosphere, *Bull. Amer. Meteor. Soc.*, *79*(10), 2101–2114, doi:10.1175/1520-0477(1998)079⟨2101:SARATS⟩2.0.CO;2.

Stroeve, J., M. Serreze, S. Drobot, S. Gearheard, M. Holland, J. Maslanik, W. Meier, and T. Scambos (2008), Arctic sea ice extent plummets in 2007, *Eos Trans. AGU*, *89*(2), 13–20, doi:10.1029/2008EO020001.

Wang, W., and P. H. Stone (1980), Effect of ice-albedo feedback on global sensitivity in a one-dimensional radiative-convective climate model, *J. Atmos. Sci.*, *37*(3), 545–552, doi:10.1175/1520-0469(1980)037⟨0545:EOIAFO⟩2.0.CO;2.

S. R. Hudson, Norwegian Polar Institute, Fram Centre, N-9296 Tromsø, Norway. (hudson@npolar.no)